Proceedings of 2018 IEEE
International Conference on Mechatronics and Automation
August 5 - 8, Changchun, China

Modeling and Analysis of a Variable Stiffness Actuator for a Safe Home-based Exoskeleton

Yi Liu [*1], Shuxiang Guo [*2*3], Songyuan Zhang[*1] and Luc Boulardot[*1]

[*1] Graduate School of Engineering
[*2] Department of Intelligent Mechanical Systems Engineering

Kagawa University
Hayashi-cho, Takamatsu, 761-0396, Japan

s18d504@stu.kagawa-u.ac.jp

[*3] Key Laboratory of Convergence Medical Engineering System and Healthcare Technology,
The Ministry of Industry and Information Technology,
School of Life Science

Beijing Institute of Technology
Haidian District, Beijing, 100081, China

guo@eng.kagawa-u.ac.jp

***Abstract* –In this paper, we modelled and analyzed a variable stiffness actuator-based exoskeleton which could provide optimal actuated elbow stiffness for those patients with a specific impairment of upper limbs. In this exoskeleton, a variable stiffness actuator is integrated for adjusting the actuated joint stiffness independently. Stiffness adjustment is realized based on a movable pivot to change the transmission ratio between the elastic elements and the output link. The characteristic of the elastic elements affects the performance of the variable stiffness actuator. Therefore, we established the model of the variable stiffness actuator and simulated its stiffness characteristics with different spring coefficients, preloads and damping respectively. We analyzed how those factors affect the characteristics of the proposed variable stiffness actuator. The performance of the variable stiffness actuator-based exoskeleton could be improved by properly choosing the spring parameters.**

Index Terms – Spring characteristic, Exoskeleton, Safety, Variable stiffness actuator

I. Introduction

The incidence rate of the stroke has increased continuously in recent years [1]. Stroke is a leading reason of the disabilities, which always leads to the impairment of upper limb and disabilities of performing activities of daily living (ADLs) [2]. After the outbreak of this disease, it is extremely important for those patients to perform rehabilitation training timely and intensively. However, due to the limitation of therapists and medical resources, many stroke patients cannot acquire professional and effective rehabilitation training.

Therefore, robot-aided rehabilitation systems have been proposed to relieve the burden of therapists and support patient's ADLs [3]-[8]. Compared with traditional physician therapies, robot-aided rehabilitation training could realize concrete motor function evaluation based on the data such as residual voluntary joint force and muscle strength collected by sensors [9]. Concerned clinical studies have verified the robot-assisted movement training could decrease impairment and improve muscular strength more significantly rather than conventional therapies [10]. To relieve patients from exhausting round-trips between home and the rehabilitation center, some home-based rehabilitation systems have been proposed [11]-[19]. They are charaterized by light-weight, low-cost and easily applied at home. In our Lab., Song et al. developed a novel upper limb exoskeleton rehabilitation device (ULERD) for realizing home-based rehabilitation training and implemented bilateral training movements of upper limbs by the aid of a commercial haptic device (Phantom Premium, 3D Systems, Inc., U.S.A.) [20]. In the following study, a human-machine synchronization control was presented for active rehabilitation training [21]. In addition, continuous upper limb motion recognition methods based on surface electro-mygraphy (sEMG) signals were applied to drive ULERD for bilateral rehabilitation training [22]. Moreover, muscle strength assessment system was establisded based on sEMG signals to predict the muscle force of the patients [23].

For a wearable exoskeleton which interacts closely with the wearer, its actuation system should ensure a safe patient-robot interaction when emergencies occur. Stroke patients often suffer severe spasms, i.e. an involuntary contraction of muscles. When using stiff actuators, undesired motions such as those caused by spasms will lead to large interaction forces between human and exoskeletal joints during movements and thus threaten the user's safety. Besides, stiff actuation always cause discomfort to the users when the robot drives his/her upper limb to complete movements. Adding compliance to the actuation system can naturally absorb the interaction force and thus prevent potential damage to the user's limbs as well as improving wearing comfort although there are increasing position errors. Therefore, compliant actuators are widely applied in rehabilitation devices. They can be mainly divided into two kinds: active compliant actuators and passive compliant actuators. For active compliant actuators which mimic the behavior of the spring, the compliance is realized by the closed loop feedback which relies on proper sensors. The bandwidth of the active compliance controller is limited and the compliance adjustment will lose effect once those sensors failed, thus a safe human-robot interaction cannot be guaranteed. Besides, continuous energy dissipation is a main problem in the active compliant actuators. Different from closed-loop controlled active compliant actuators, passive compliant actuators realize the compliance of the actuation by mounting elastic elements between the motor and the actuated load. Hence, the compliance is an inherent hardware property benefitted by the elastic elements. Series elastic actuator

(SEA) was adopted in the rehabilitation devices to ensure a safe human-robot interaction during rehabilitation task [24]-[26]. However, the physical compliance of SEA is a fixed value which is related to the coefficient of the spring elasticity. To overcome these limitations, variable stiffness actuators (VSAs) have been proposed [27]. VSAs could minimize large interaction forces caused by shocks or spasms to ensure a safe interaction between the user and the exoskeleton in low stiffness while realizing precise position control or trajectory movements in high stiffness. VSAs mainly rely on the internal elastic elements to realize variable stiffness passively and don't need additional controllers. Therefore, the characteristics of the internal elastic elements play an important role in the VSAs. In this paper, we simulated how the factors of the elastic elements affect the performance of the proposed exoskeleton.

The rest of this paper is organized by the following sections. The VSA-based exoskeleton is introduced in Section II. Characteristic analysis of the internal elastic elements could be seen in Section III. Finally, conclusions are given in Section IV.

II. Methods

A. Overview of the Variable Stiffness Actuator-based Exoskeleton

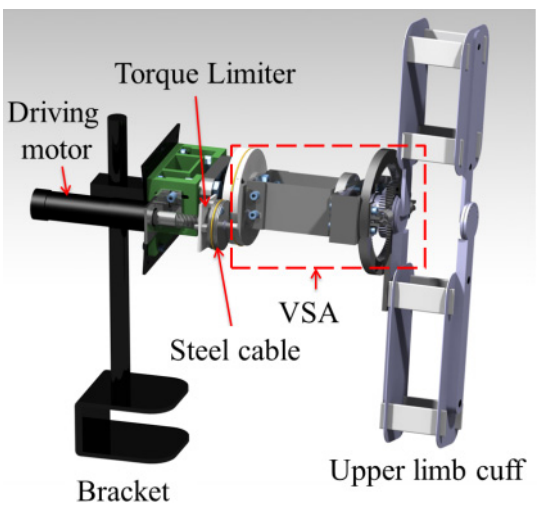

Fig. 1 Mechanical Design of the VSA-based Exoskeleton

TABLE I
PARAMETERS OF MOTORS

Motor	RE-30	EC max-16
Type power	60 W	8 W
Nominal voltage	12 V	6 V
No load speed	7480 rpm	12000 rpm
Nominal torque	51.7 mNm	7.66 mNm

TABLE II
PARAMETERS OF GEARHEADS

Gearhead	GP 32 C	GP 16 C
Reduction	190:1	84:1
Max. continuous torque	6 Nm	0.3 Nm

The mechanical design of the proposed exoskeleton is shown in Fig. 1. It mainly consists of a fixed bracket, a driving motor for elbow rotation, a torque limiter to avoid any overload, an integrated VSA to adjust the stiffness of the elbow joint and a cuff for upper limb. Different from traditional exoskeletons which are bulky and heavy, the proposed exoskeleton is light-weight and easy to be worn. Besides, it could realize passive rehabilitation training (robot-in-charge) and active rehabilitation training (patient-in-charge) for the elbow rehabilitation training [17]. The flexion and extension of the elbow joint is powered by a Maxon motor (Maxon RE-30 Graphite Brushes Motor, Switzerland). It is connected to a planetary gearhead (Maxon GP 32 C) of which the reduction ratio is 190:1. By the combination of this high-power-density motor and the gearhead with a high reduction ratio, the exoskeleton could provide enough force/torque to assist patients to complete elbow rehabilitation tasks. A steel cable with a diameter of 1mm is adopted to transmit the motor power.

As a home-based wearable power-assist exoskeleton which interacts closely with the user, its actuation system should guarantee a comfortable and safe human-robot interaction even emergencies occur. For those patients with severe impaired upper limbs, the exoskeleton could drive the patient's arm to complete rehabilitation tasks in low actuated stiffness. When they regained a partial control ability of their upper limbs, the user could perform rehabilitation movements with a high trajectory precision in high stiffness. In this exoskeleton, a VSA is integrated to adjust the stiffness of the actuated elbow joint. The stiffness variation is realized by moving a pivot along the lever. A Maxon EC max-16 motor equipped with a planetary gearbox GP 16C is used to move the pivot position. The parameters of the motors and gearheads could be seen in Table I and Table II respectively.

B. Structure and Working Principle of the VSA

Different methods based on elastic elements have been proposed to realize variable stiffness passively. They can be categorized into: (1) Equilibrium-controlled stiffness which applies a fixed stiffness spring in series with a stiff actuator (2) Antagonistic-controlled stiffness of which two actuators with non-adaptable compliance and nonlinear force-displacement characteristics are coupled antagonistically (3) Structure-controlled stiffness which modulates the effective physical structure of a spring to achieve variations in stiffness (4) Mechanical-controlled stiffness which adjusts the effective physical stiffness of the system. They realized variable stiffness by changing the pretension of the internal elastic elements.

Most of equilibrium-controlled devices have complicated structures for the purpose of realizing variable stiffness. And many antagonistic-controlled stiffness devices are designed with two antagonistic non-linear springs, which are difficult for dimensioning and regulating. Although there are some devices without springs but equipped with a magnetic, hydraulic or pneumatic VSAs, they are difficult to be applied in home-based exoskeletons because of size, cost and complexity. To overcome these limitations, a compact and light-weight VSA is equipped in the proposed exoskeleton. It has the following

features: 1) large range of variable stiffness to meet the requirements of different training tasks; 2) simple structure with small size which can be easily integrated into the exoskeleton system; 3) low power consumption for a long operation.

The structure of the proposed VSA could be seen in Fig. 2. It consists of a pair of antagonistic springs, a movable pivot and an output link. The pivot is moved by a planetary gear mechanism, which could realize a straight motion of the pivot by rotation, thereby decrease the friction during pivot movement [28].

The proposed variable stiffness mechanism could be simplified as shown in Fig. 3. There is an actuated load at the end of the output link, while the other side is tensioned with a pair of antagonistic springs. The actuated force could rotate the lever arm to generate a deflection which will lead to the spring elongation. The force due to spring elongation will balance the actuated force via the lever. In addition, a pivot could move along the lever. As long as the position of the pivot is changed, the transmission ratio of the elastic elements versus output end will be changed as well. Based on the equilibrium of moments, to rotate the same deflection δ, the force exerted on the output end will be varied according to the transmission ratio. The output stiffness K, is defined as

$$K = \frac{F}{\delta} \tag{1}$$

where F is the force exerted on the end of output link and δ is the output deflection along the orientation under the action of force.

Therefore, the stiffness variation is implemented by moving the pivot position. By this way, variable stiffness is an inherent characteristic related to the pivot position. Compared with those active impedance controls [29], this kind of adjustment method is more reliable and could minimize the risk of instabilities caused by the control system. Besides, the stiffness variation could be achieved without energy injection into or extraction from the internal elastic elements. In other words, all the energy provided by the motor can be used to adjust the stiffness of the elbow joint without energy loss caused by inertial elastic elements. In addition, this variable stiffness mechanism can be integrated to the forearm part of the exoskeleton due to its compact structure.

The schematic diagram of the different stiffness settings is shown in Fig. 4. By moving the position of the pivot along the lever arm, the actuated stiffness of the elbow joint could be adjusted to adapt to the patients with a specific impairment of upper limb.

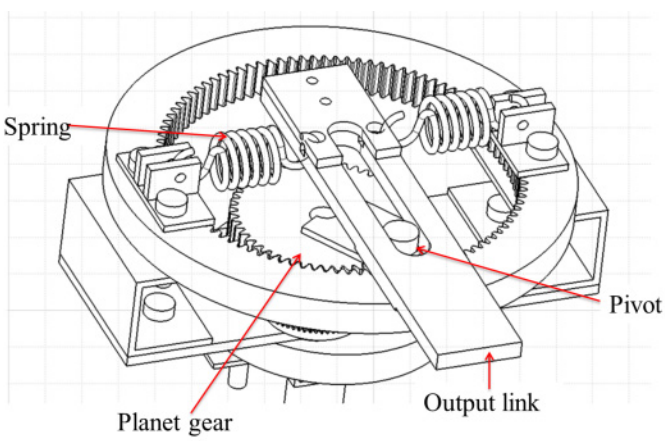

Fig. 2 Structure of the VSA

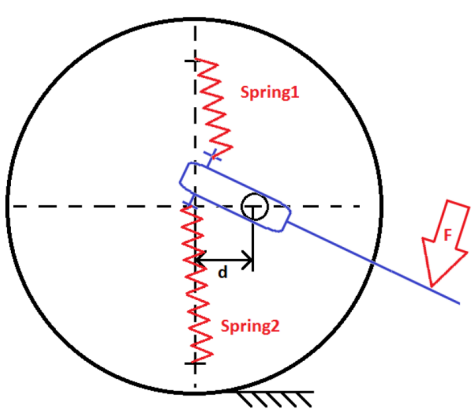

Fig. 3 Working Principle

III. Modeling and Analysis

The stiffness variation of the exoskeleton device is realized based on the internal elastic elements (tensioned springs), which have significant effects on the performance of the passive VSAs. Therefore, we established the dynamic model in Adams software (MSC Software, Mechanical Dynamics Inc., U.S.A.) as shown in Fig. 5 and simulated how the spring characteristics affect the stiffness variation. The spring preload, damping and spring coefficients are analyzed respectively.

During the simulation process, a force with a constant increment of 1N/s (i.e., F=1*time (s)) is exerted on the end of the output link. The output link will be rotated from its equilibrium position and generate a deflection as shown in Fig. 6.

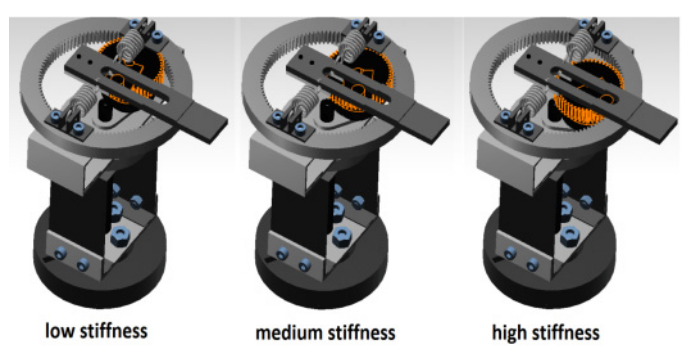

Fig. 4 Different stiffness settings by moving the pivot position

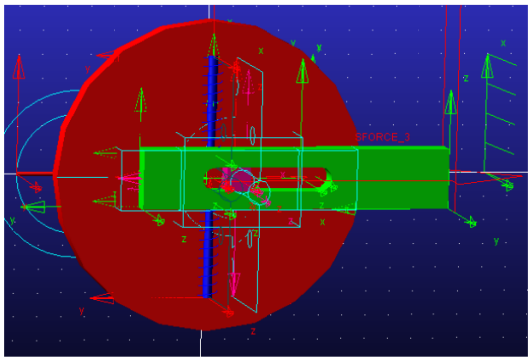

Fig. 5 Established Dynamic Model

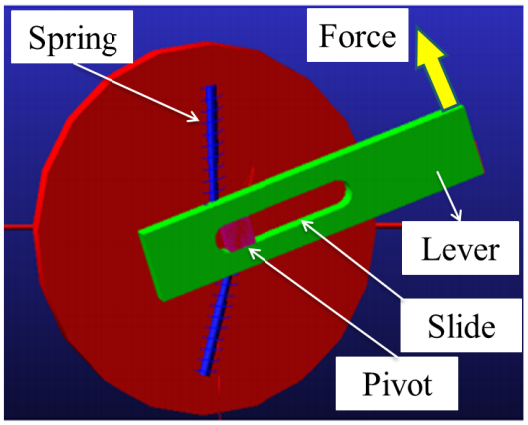

Fig. 6 Dynamic simulation

A. *Spring Preload*

In this case, the pivot position d is located at 20mm away from the spring and the coefficient of spring elasticity is 19.6 N/mm. The damping coefficient is set as 10 Ns/mm. The preload of the springs was varied to explore its effect on stiffness variation. The simulation result could be seen in Fig. 7. The negative value of the preload represents that the spring is in traction, while the positive value of the preload represents that the spring is in compression. The initial preload is 20 N and be changed with an increment of -20 N for each curve.

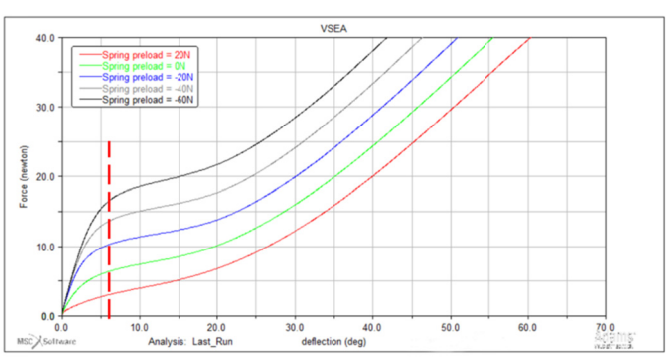

Fig. 7 Force-deflection Diagram for different spring preloads

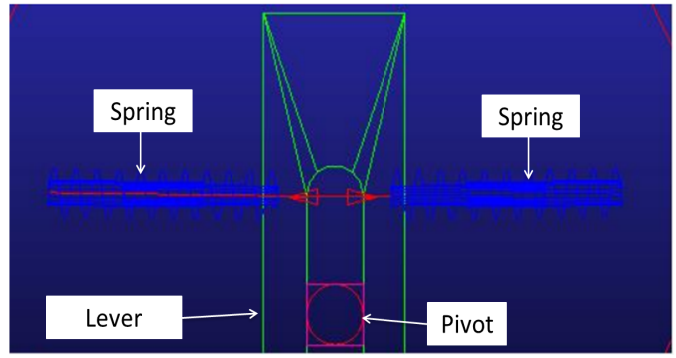

(a) Two springs are in traction

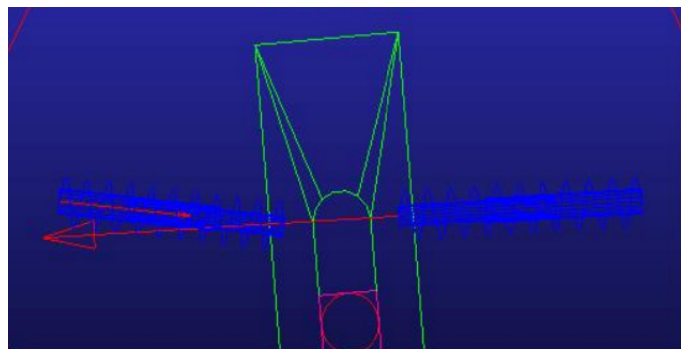

(b) The left spring is released, while the right spring is elongated

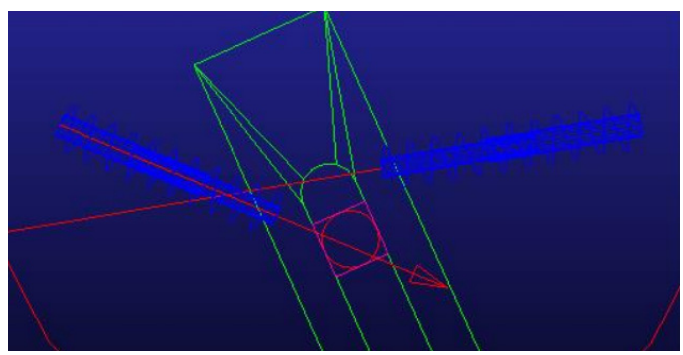

(c) Both of the two springs are elongated

Fig. 8 Schematic Diagram of spring variations

From the result, we can see there is an inflection point in each curve, which means a stiffness variation. The red dashed line divided each curve into 2 stages according to the slope. The phenomenon results from the configuration of the antagonistic springs which can be explained by Fig. 8. The initial state of the VSA, where two springs are in traction due to their preload, is shown in Fig. 8 (a). The red arrows represent the spring forces. The external force is exerted on the output link, which leads to a deflection from its equilibrium position. Assumed that the output link is rotated by following clockwise direction, the spring in the left side is released and that in the right side is elongated. Therefore, the spring force on the left is decreased while the spring force on the right is increased. Fig. 8 (b) shows the moment of smallest spring force on the left side. When the deflection of the output link continue to increase, the left spring will be elongated as

well. As shown in Fig. 8 (c), both of the two springs are elongated but their spring forces are opposite. Hence, the slope in the second stage is slower than that in the first stage. According to the definition of stiffness K=F/δ, the slope of the force-deflection diagram represents its stiffness. Hence, the stiffness is decreased after the inflection point.

It can be observed in Fig. 7 that increasing the preload of the spring could significantly change the stiffness in the first stage. After the inflection point occurs, the slope in the second stage is almost the same for each curve, which means the same stiffness in the second stage. Hence, the preload of the springs can only change the stiffness of the first stage and doesn't affect the stiffness in the second stage.

B. *Damping coefficient*

In this case, the pivot position d is located at 10mm away from the springs. The coefficient of spring elasticity is chosen as 19.6 N/mm and the preload of springs is set as 40 N. The damping coefficient was varied to see its effect on the stiffness variation.

The simulation result can be seen in Fig. 9. From Fig. 9 (a), when the damping coefficient varied from 0.1 to 40 Ns/mm, the curves have similar shapes although there is a small deviation. It can be observed that the slope of each curve in force-deflection diagram is almost the same when the deflection is larger than 6°. The variation of damping coefficient is not an essential factor for the VSA when the pivot position is 10 mm. However, when we zoomed in small range of deflection, it can be noticed in Fig. 9 (b) that vibrations occurred if the damping coefficient is too small. Hence, in order to guarantee the stability of VSA, the minimum damping coefficients of the VSA should be larger than 2 Ns/mm.

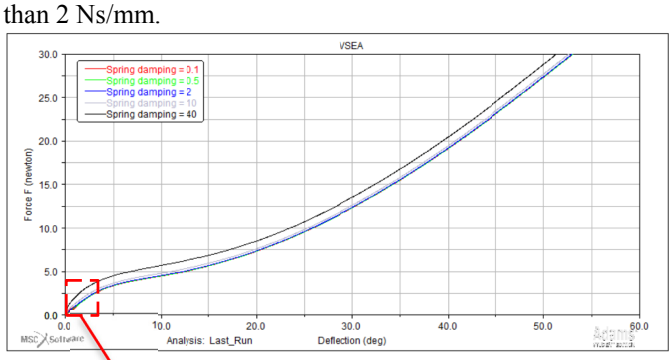

(a) Whole Range of Deflection (0-60°)

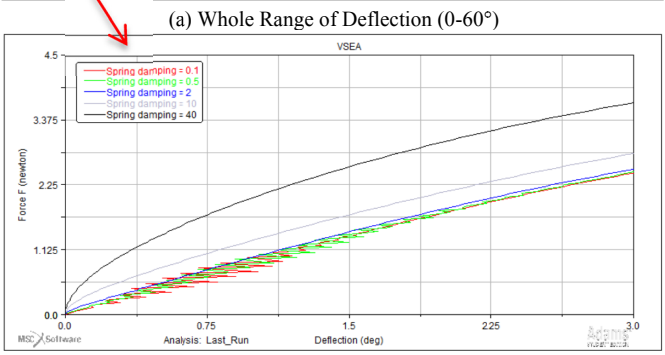

(b) Zoom in Small Deflection Range (0-3°)

Fig. 9 Force-deflection Diagram for different damping values (Pivot position =10 mm)

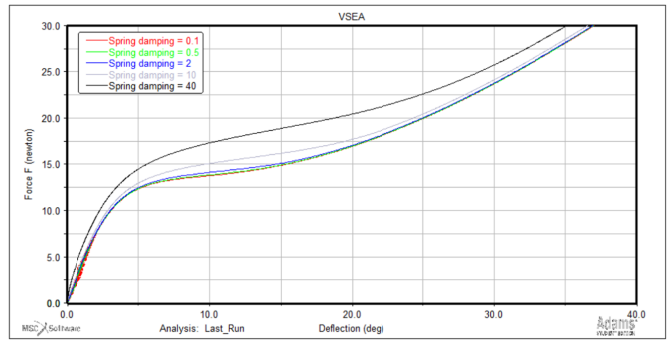

Fig. 10 Force-deflection Diagram for different damping values (Pivot position =20 mm)

The pivot position was moved to 20mm to observe the behavior of the damping coefficients in a higher stiffness. The simulation result for different damping coefficients could be seen in Fig. 10. When the damping coefficient varied from 0.1 to 10 Ns/mm, the force-deflection diagram of each curve is similar. However, the difference between damping coefficient 40 Ns/mm and others is enlarged. The high damping always lead to a severe energy dissipation of the system. This phenomenon becomes notable when the pivot position increased. The simulation results revealed the damping coefficient has limited influence on the performance of the VSA. But a minimum damping coefficient is required to avoid vibrations of the system. And high damping coefficient may result in severe energy dissipation in the VSA. Thanks to the simulation result, the damping coefficient is preferred to be chosen from 2 to 10 Ns/mm.

C. *Spring coefficient K*

In this case, the pivot position d is located at 20mm away from the spring and the preload of the spring is -40 N. The damping coefficient is set as 10 Ns/mm. The spring coefficient was varied to see its effect on stiffness variation. The simulation result could be seen in Fig. 11. As we can see, to achieve the same deflection, the exerted force is increased with the increase of the spring coefficient. The stiffness of the VSA could be increased both in the first and second stages by choosing a higher spring coefficients.

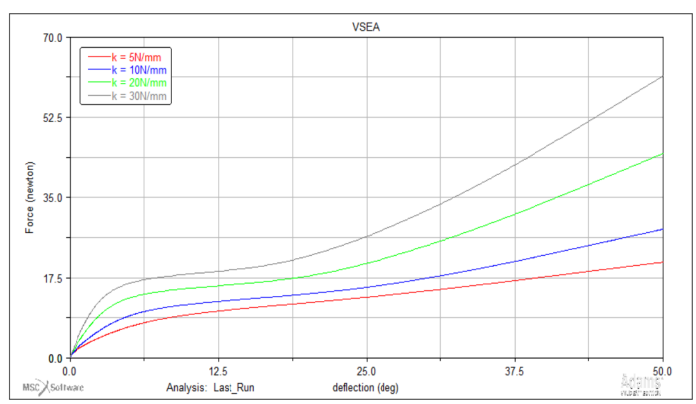

Fig. 11 Force-deflection Diagram for different spring coefficients

IV. Conclusions

In this paper, a VSA-based exoskeleton for safe home-based rehabilitation training has been introduced. It could adjust the actuated joint stiffness to adapt to the patient with a specific impairment of upper limbs. The internal springs affect the inherent stiffness of the VSA. In this paper, we analyzed the related spring characteristics by simulations. The results showed the spring preload could only change the stiffness in the first stage, but have no effect on the second stage. Spring coefficient could change the stiffness in both stages. Although damping value has no significant influence on the stiffness variation, a suitable range of damping value is needed to avoid vibrations of the system and excessive energy dissipation. Based on the analysis above, an optimal combination of spring characteristics is desired to improve the performance of the proposed VSA-based exoskeleton.

Acknowledgment

This research is partly supported by National High Tech. Research and Development Program of China (No.2015AA043202), and SPS KAKENHI Grant Number 15K2120.

References

[1] D. Mozaffarian, E. J. Benjamin, A. S. Go, D. K. Arnett, M. J. Blaha, M. Cushman, *et al.*, "Executive summary: Heart Disease and Stroke Statistics-2016 update: A report from the American Heart Association", *Circulation,* vol. 133, no. 4, p. 447, 2016.

[2] S. Barreca, S. L. Wolf, S. Fasoli, and R. Bohannon, "Treatment interventions for the paretic upper limb of stroke survivors: a critical review", *Neurorehabilitation and neural repair,* vol. 17, no. 4, pp. 220-226, 2003.

[3] M. Babaiasl, S. H. Mahdioun, P. Jaryani, and M. Yazdani, "A review of technological and clinical aspects of robot-aided rehabilitation of upper-extremity after stroke," *Disability and Rehabilitation: Assistive Technology,* vol. 11, no. 4, pp. 263-280, 2016.

[4] Y. Hsieh, T. Shih, K. Lin, and C. Wu, "Upper-extremity robot-aided rehabilitation after stroke: A comparison of the arm and wrist robots," *Journal of the Neurological Sciences,* vol. 381, p. 599, 2017.

[5] J. M. Veerbeek, A. C. Langbroek-Amersfoort, E. E. van Wegen, C. G. Meskers, and G. Kwakkel, "Effects of robot-assisted therapy for the upper limb after stroke: a systematic review and meta-analysis," *Neurorehabilitation and neural repair,* vol. 31, no. 2, pp. 107-121, 2017.

[6] N. Smania, N. Valè, E. Dimitrova, S. Mazzoleni, M. Filippetti, C. Depaoli, *et al.*, "Effects of high-intensity robot-assisted training in hand function recovery and adl independence in individuals with multiple sclerosis: A randomized controlled single-blinded trial," *Gait & Posture,* vol. 57, p. 16, 2017.

[7] Y. Hsieh, C. Wu, W. Wang, K. Lin, K. Chang, C. Chen, *et al.*, "Bilateral robotic priming before task-oriented approach in subacute stroke rehabilitation: A pilot randomized controlled trial," *Clinical rehabilitation,* vol. 31, no.2, pp. 225-233, 2017.

[8] C. Lauretti, F. Cordella, E. Guglielmelli, and L. Zollo, "Learning by Demonstration for planning activities of daily living in rehabilitation and assistive robotics," *IEEE Robotics and Automation Letters,* vol. 2, no.3, pp. 1375-1382, 2017.

[9] N. Vitiello, T. Lenzi, S. Roccella, S. M. De Rossi, E. Cattin, F. Giovacchini, *et al.*, "NEUROExos: A powered elbow exoskeleton for physical rehabilitation," *IEEE Transactions on Robotics,* vol. 29, no. 1, pp. 220-235, 2013.

[10] S. Hesse, G. Schulte-Tigges, M. Konrad, A. Bardeleben, and C. Werner, "Robot-assisted arm trainer for the passive and active practice of bilateral forearm and wrist movements in hemiparetic subjects," *Archives of physical medicine and rehabilitation,* vol. 84, no. 6, pp. 915-920, 2003.

[11] Z. Song, S. Guo, M. Pang, and S. Zhang, "Recognition of motion of human upper limb using semg in real time: Towards bilateral rehabilitation," in *Proceedings of 2012 IEEE International Conference on Robotics and Biomimetics (ROBIO)*, pp. 1403-1408, 2012.

[12] S. Zhang, S. Guo, M. Pang, and M. Qu, "Training model-based masterslave rehabilitation training strategy using the phantom Premium and an exoskeleton device," in *Proceedings of 2014 International Conference on Complex Medical Engineering*, pp. 26-29, 2014.

[13] Z. Song, S. Guo, M. Pang, S. Zhang, N. Xiao, B. Gao, et al., "Implementation of resistance training using an upper-limb exoskeleton rehabilitation device for elbow joint", *Journal of Medical and Biological Engineering*, vol. 34, no. 2, pp. 188-196, 2014.

[14] S. Zhang, S. Guo, M. Pang, B. Gao, and P. Guo, "Mechanical design and control method for sea and VSA-based exoskeleton devices for elbow joint rehabilitation," *Neuroscience and Biomedical Engineering,* vol. 2, no. 3, pp. 142-147, 2014.

[15] S. Zhang, S. Guo, B. Gao, H. Hirata, and H. Ishihara, "Design of a Novel Telerehabilitation System with a Force-Sensing Mechanism," *Sensors*, vol. 15, no. 5, pp. 11511-11527, 2015.

[16] S. Zhang, S. Guo, B. Gao, Q. Huang, M. Pang, H. Hirata, *et al.*, "Muscle Strength Assessment System Using sEMG-Based Force Prediction Method for Wrist Joint," *Journal of Medical and Biological Engineering,* vol. 36, no. 1, pp. 121-131, 2016.

[17] S. Zhang, S. Guo, Y. Fu, L. Boulardot, Q. Huang, H. Hirata, et al., "Integrating Compliant Actuator and Torque Limiter Mechanism for Safe Home-Based Upper-Limb Rehabilitation Device Design," *Journal of Medical and Biological Engineering*, vol. 37, no. 3, pp. 357-364, 2017.

[18] Y. Liu, S. Guo, S. Zhang, and L. Boulardot, "A novel sEMG control-based variable stiffness exoskeleton," In Proceedings of *2017 IEEE International Conference on Mechatronics and Automation (ICMA),* pp. 1444-1449, 2017.

[19] Z. Song, S. Guo, and Y. Fu, "Development of an upper extremity motor function rehabilitation system and an assessment system," International Journal of Mechatronics and Automation, vol. 1, no. 1, pp. 19-28, 2011.

[20] Z. Song and S. Guo, "Design process of exoskeleton rehabilitation device and implementation of bilateral upper limb motor movement," *Journal of Medical and Biological Engineering*, vol. 32, no. 5, pp. 323-330, 2012.

[21] Z. Song, S. Guo, N. Xiao, B. Gao, and L. Shi, "Implementation of human-machine synchronization control for active rehabilitation using an inertia sensor," *Sensors*, vol. 12, no. 12, pp. 16046-16059, 2012.

[22] M. Pang, S. Guo, and Z. Song, "Study on the sEMG driven upper limb exoskeleton rehabilitation device in bilateral rehabilitation," *Journal of Robotics and Mechatronics*, vol. 24, no.4, p. 585, 2012.

[23] S. Guo, M. Pang, B. Gao, H. Hirata, and H. Ishihara, "Comparison of sEMG-based feature extraction and motion classification methods for upper-limb movement," *Sensors*, vol. 15, no. 4, pp. 9022-9038, 2015.

[24] H. Yu, S. Huang, G. Chen, Y. Pan, and Z. Guo, "Human–robot interaction control of rehabilitation robots with series elastic actuators," *IEEE Transactions on Robotics,* vol. 31, no. 5, pp. 1089-1100, 2015.

[25] L. H. Blumenschein, C. G. McDonald, and M. K. O'Malley, "A cable-based series elastic actuator with conduit sensor for wearable exoskeletons," in Proceedings of *2017 IEEE International Conference on Robotics and Automation (ICRA),* pp. 6687-6693, 2017.

[26] X. Li, Y. Pan, G. Chen, and H. Yu, "Adaptive human–robot interaction control for robots driven by series elastic actuators," *IEEE Transactions on Robotics,* vol. 33, no. 1, pp. 169-182, 2017.

[27] S. Wolf, G. Grioli, O. Eiberger, W. Friedl, M. Grebenstein, H. Höppner, *et al.*, "Variable stiffness actuators: Review on design and components," *IEEE/ASME transactions on mechatronics,* vol. 21, no. 5, pp. 2418-2430, 2016.

[28] S. S. Groothuis, G. Rusticelli, A. Zucchelli, S. Stramigioli, and R. Carloni, "The variable stiffness actuator vsaut-ii: Mechanical design, modeling, and identification," *IEEE/ASME transactions on mechatronics,* vol. 19, no. 2, pp. 589-597, 2014.

[29] C. Semini, V. Barasuol, T. Boaventura, M. Frigerio, M. Focchi, D. G. Caldwell, *et al.*, "Towards versatile legged robots through active impedance control," *The International Journal of Robotics Research,* vol. 34, no. 7, pp. 1003-1020, 2015.